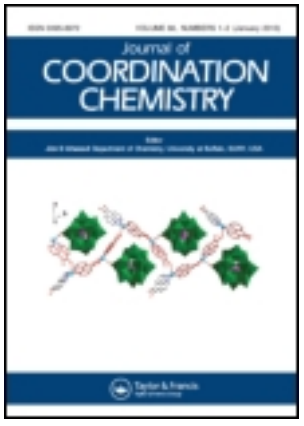

Journal of Coordination Chemistry
Publication details, including instructions for authors and subscription information:
http://www.tandfonline.com/loi/gcoo20

Syntheses, urease inhibition activities, and fluorescent properties of transition metal complexes

Xiaoyang Qiu [a], Jing Wang [a], Dahua Shi [b], Suzhi Li [a], Fuli Zhang [a], Fuqiang Zhang [a], Guangxiu Cao [a] & Bin Zhai [a]

[a] Engineering Research Center of Functional Material Preparation, Shangqiu Normal University, Shangqiu, P.R. China

[b] School of Chemical Engineering, Huaihai Institute of Technology, Lianyungang, P.R. China

Accepted author version posted online: 21 Mar 2013.Published online: 29 Apr 2013.

To cite this article: Xiaoyang Qiu, Jing Wang, Dahua Shi, Suzhi Li, Fuli Zhang, Fuqiang Zhang, Guangxiu Cao & Bin Zhai (2013) Syntheses, urease inhibition activities, and fluorescent properties of transition metal complexes, Journal of Coordination Chemistry, 66:9, 1616-1625, DOI: 10.1080/00958972.2013.787144

To link to this article: http://dx.doi.org/10.1080/00958972.2013.787144

Journal of Coordination Chemistry, 2013
Vol. 66, No. 9, 1616–1625, http://dx.doi.org/10.1080/00958972.2013.787144

Syntheses, urease inhibition activities, and fluorescent properties of transition metal complexes

XIAOYANG QIU*†, JING WANG†, DAHUA SHI‡, SUZHI LI†, FULI ZHANG†, FUQIANG ZHANG†, GUANGXIU CAO† and BIN ZHAI*†

†Engineering Research Center of Functional Material Preparation, Shangqiu Normal University, Shangqiu, P.R. China
‡School of Chemical Engineering, Huaihai Institute of Technology, Lianyungang, P.R. China

(*Received 3 December 2012; in final form 22 January 2013*)

Four transition metal complexes with Schiff base and 1,10-phenanthroline, $[Cu(L)(phen)]_2 \cdot C_2H_5OH$ (**1**), $[Zn(L)(phen)]_2 \cdot C_2H_5OH$ (**2**), $[Ni(L)(phen)]_2 \cdot C_2H_5OH$ (**3**), and $[Co(L)(phen)]_2 \cdot C_2H_5OH$ (**4**) (H_2L = 1-((2-hydroxynaphthalen-1-yl)methylene)thiosemicarbazide; phen = 1,10-phenanthroline) were synthesized and characterized by physico-chemical methods. The crystal structure of **1** was determined by X-ray single-crystal diffraction analysis. **1** crystallizes in the orthorhombic space group *Pbca* with $a = 15.008(9)$, $b = 16.100(10)$, $c = 37.54(2)$ Å, $V = 9070(10)$ Å^3, $Z = 8$, $GOOF = 1.002$, $R_1 = 0.0626$, and $wR_2 = 0.0912$. The fluorescence and urease inhibitory activities of the compounds were tested. The enzymatic activity study indicated that **3** possessed potent inhibition against *jack bean* urease, with $IC_{50} = 1.2 \pm 0.1$ μM, and about 35 times more than 42.1 ± 0.4 acetohydroxamic acid as positive reference. This suggests that inhibitory efficiency of these complexes can be strongly influenced by different transition metal ions.

Keywords: Transition metal complexes; Mixed ligands; Fluorescent properties; Urease inhibition activities

1. Introduction

Urease, the first crystallized enzyme-possessing nickel ions [1], is an important enzyme in both medicine and agriculture, rapidly catalyzing the hydrolysis of urea to form ammonia and carbamate [2–5]. The resulting carbamate spontaneously decomposes to yield second ammonia and carbon dioxide. High concentration of ammonia arising from these reactions, as well as the accompanying pH elevation has important negative implications in both human and animal health, such as causing urolithiasis, pyelonephritis, peptic ulcers, stomach cancer, etc. [6–8]. In agriculture, the efficiency of soil nitrogen fertilization with urea decreases due to ammonia volatilization and root damage caused by soil pH increase [9]. Control of the activity of urease through the use of inhibitors could counteract these negative effects.

*Corresponding authors. Email: qiuxiaoyang12@163.com; zhaibin_1978@163.com

Over the past decade, numerous compounds have been patented or proposed as inhibitors of urea hydrolysis. The urease inhibitors can be broadly classified into two fields: (1) organic compounds, such as hydroxamic acid [10], phosphoramidates [11, 12], triazole [7, 13], and benzoquinone [14]; (2) metal complexes, such as copper(II), zinc(II), manganese(II), and cadmium(II) complexes [15–21]. Among known urease inhibitors, hydroxamic acids are the best recognized urease inhibitors [10]. However, their application as a drug *in vivo* is limited because of the teratogenicity of hydroxamic acid in rats [22] and the degradation of phosphoramidates at low pH [23]. Some complexes based on Schiff bases have shown significant inhibitory activity against urease and have aroused considerable interest [15–17, 19, 24]. We have recently reported the biological activity of some complexes with Schiff bases [25–29]. Considering metal complexes with Schiff bases are versatile enzyme inhibitors, four Schiff base transition metal complexes with 1,10-phenanthroline (phen), $[Cu(L)(phen)]_2 \cdot C_2H_5OH$ (**1**), $[Zn(L)(phen)]_2 \cdot C_2H_5OH$ (**2**) $[Ni(L)(phen)]_2 \cdot C_2H_5OH$ (**3**), and $[Co(L)(phen)]_2 \cdot C_2H_5OH$ (**4**), where L is the deprotonated form of 1-((2-hydroxynaphthalen-1-yl)methylene)thiosemicarbazide (H_2L), were prepared and structurally characterized. Urease inhibitory activity and fluorescence of the complexes were also investigated.

2. Experimental

2.1. *Materials and measurements*

Urease (from jack beans, type III, activity 22 units/mg solid), HEPES (Ultra) buffer, and urea (Molecular Biology Reagent) were from Sigma. All other reagents and solvents were purchased from commercial suppliers and used without purification. Elemental analyses for C, H, and N were carried out on a Perkin–Elmer 2400 analyzer. FT-IR spectra were recorded using KBr pellets (4000–400 cm^{-1}) on a Nexus 870 FT-IR spectrophotometer. UV–vis spectra from 200 to 800 nm were measured in DMSO/H_2O (1 : 1 v/v) solution on a 760 CRT UV–vis spectrophotometer from Shanghai Precision Instrument Corporation. Fluorescence spectra were recorded on a Shimadzu RT-5301PC fluorescence spectrophotometer.

2.2. *Synthesis of H_2L*

Thiosemicarbazide (0.91 g, 10.0 mmol) was dissolved in 50 mL of EtOH/H_2O hot mixture (1:1 v/v) and 2-hydroxyl-1-naphthaldehyde (1.72 g, 10.0 mmol) in 50 mL of the EtOH/H_2O mixture was slowly added to the above mixture. After being refluxed for 4 h, the yellow precipitates were filtered off, washed with EtOH, and dried in air. Yield: 78%. Anal. Calcd for $C_{12}H_{11}N_3OS$: C, 58.8; H, 4.5; N, 17.1. Found: C, 58.6; H, 4.4; N, 17.3%. IR (KBr, cm^{-1}): 3444, 3258, 3162, 1608, 1519, 1465, 1392, 1323, 1276, 1237, 1185, 1117, 950, 819, 748, 645, 600, 487, 446. UV–vis [DMSO–H_2O (1 : 1 v/v), λ/nm]: 365, 330, 265.

2.3. *Synthesis of 1–4*

Complexes **1**–**4** were prepared by similar synthetic methods. H_2L (0.5 mmol) was dissolved in 50 mL of the EtOH/H_2O mixture by stirring and heating. An equimolar amount of transition metal acetate was dissolved in 20–50 mL of the same solvent mixture and an equimolar amount of phen was dissolved in 20 mL of EtOH. The latter two were

added to the ligand solution. The resulting mixture was stirred at 50–60 °C for 30 min. By evaporation of the solvent, single crystal for **1** and precipitates for **2**–**4** were obtained. The products were filtered off, washed with EtOH, and dried in a vacuum desiccator containing anhydrous $CaCl_2$.

Complex **1**
Black-green solid, Yields: 47%. Anal. Calcd for $C_{50}H_{40}Cu_2N_{10}O_3S_2$: C, 58.8; H, 4.5; N, 17.1. Found: C, 58.6; H, 4.4; N, 17.3%. FT-IR (KBr, cm^{-1}): 3335, 3111, 1613, 1500, 1387, 1334, 1184, 1092, 1045, 960, 872, 756, 719, 625, 576, 526, 487, 600, 487, 446. UV–vis [DMSO–H_2O (1 : 1 v/v), λ/nm]: 415, 335.

Complex **2**
Orange solid, Yields: 61%. Anal. Calcd for $C_{50}H_{40}Zn_2N_{10}O_3S_2$: C, 58.7; H, 3.9; N, 13.7. Found: C, 58.4; H, 3.7; N, 13.9%. FT-IR (KBr, cm^{-1}): 3419, 3131, 1607, 1487, 1423, 1386, 1332, 1170, 1091, 1039, 954, 836, 755, 719, 684, 611, 440. UV–vis [DMSO–H_2O (1 : 1 v/v), λ/nm]: 405, 335.

Complex **3**
Brown green solid, Yields: 52%. Anal. Calcd for $C_{50}H_{40}Ni_2N_{10}O_3S_2$: C, 59.4; H, 4.0; N, 13.9. Found: C, 58.8; H, 3.7; N, 14.1%. FT-IR (KBr, cm^{-1}): 3331, 3151, 1663, 1607, 1533, 1486, 1393, 1328, 1191, 1096, 1046, 967, 832, 741, 614, 515. UV–vis [DMSO–H_2O (1 : 1 v/v), λ/nm]: 420, 385, 320.

Complex **4**
Brown black solid, Yields: 56%. Anal. Calcd for $C_{50}H_{40}Co_2N_{10}O_3S_2$: C, 59.4; H, 4.0; N, 13.9. Found: C, 59.1; H, 3.8; N, 14.2%. FT-IR (KBr, cm^{-1}): 3309, 3180, 1657, 1607, 1519, 1436, 1394, 1338, 1191, 1098, 1043, 967, 828, 749, 665, 606, 494, 447. UV–vis [DMSO–H_2O (1 : 1 v/v), λ/nm]: 430.

2.4. *X-ray crystallography*

Intensity data of **1** were collected on a Bruker Smart CCD detector using graphite monochromated Mo Kα radiation ($\lambda = 0.71073$ Å) at 296 K. The structure was solved by direct methods and refined using full-matrix least squares on F^2. All calculations were performed using the SHELXL-97 program package [30]. No hydrogens were located from the difference Fourier map and refined anisotropically. Positions of hydrogens attached to carbon and nitrogen were geometrically placed. All hydrogens were refined isotropically as a riding mode using the default SHELXTL parameters. A summary of crystal data and structure refinements for **1** is listed in table 1.

2.5. *Measurement of jack bean urease inhibitory activity*

The measurement of urease activity was carried out according to the procedure reported by Tanaka [31]. Generally, the assay mixture, containing 25 μL of *jack bean* urease (10 kU/L) and 25 μL of the tested complexes of different concentrations (dissolved in DMSO/H_2O mixture (1:1 v/v)), was preincubated for 1 h at 37 °C in a 96-well assay plate. After preincubation, 200 μL of 100 mM HEPES [*N*-(2-hydroxyethyl)piperazine-*N*′-(2-ethanesulfonic acid)] buffer pH 6.8 [32] containing 500 mM urea and 0.002% phenol red were added and incubated at 37 °C. The reaction was measured by microplate reader (570 nm), which was

Table 1. Crystallographic and experimental data for **1**.

Empirical formula	$C_{50}H_{40}Cu_2N_{10}O_3S_2$
Formula weight	1020.12
T/K	296(2)
Wavelength/Å	0.71073
Crystal shape/color	Block/black
Crystal size/mm	0.23 × 0.22 × 0.17
Crystal system	Orthorhombic
Space group	*Pbca*
a/Å	15.008(9)
b/Å	16.100(10)
c/Å	37.54(2)
V/Å^3	9070(10)
Z	8
D/g·cm^{-3}	1.494
μ(Mo Kα)/ mm^{-1}	1.086
F(0 0 0)	4192
θ range (°)	1.93–26.00
h_{min}/h_{max}	−18/18
k_{min}/k_{max}	−19/19
l_{min}/l_{max}	−46/23
Data collected	48,086
Unique data ($I > 2\sigma(I)$)	8903
Maximum and minimum transmission	0.8368 and 0.7882
Parameters	604
Restraints	12
Goodness-of-fit on F^2	1.002
R_1, wR_2 [$I > 2\sigma(I)$]	0.0626, 0.0912
R_1, wR_2 (all data)	0.1974, 0.1270
Largest difference peak and hole (e Å^{-3})	0.418 and −0.419

required to produce enough ammonium carbonate to raise the pH of a HEPES buffer from 6.8 to 7.7, the endpoint being determined by the color of phenol red indicator [15, 33].

3. Results and discussion

3.1. *Synthesis and general characterization*

The Schiff base H_2L was synthesized as yellow powder by the condensation of 2-hydroxyl-1-naphthaldehyde with thiosemicarbazide. A compound containing the thioamide, –N(H)–C(S)–, is capable of exhibiting thione/thiol tautomerism. Therefore, H_2L can exist either as the thione (1a), or as the thiol form (1b), or as an equilibrium mixture of both modes (figure 1) [34]. **1**–**4** were obtained by the reaction of $M(OAc)_2 \cdot nH_2O$ (M = Cu, Zn, Ni and Co) with mixed ligands at 50–60 °C. The analytical data for **1**–**4** are in agreement with the calculated values, though single crystals of **2**–**4** have not been obtained.

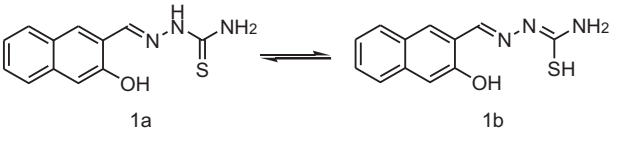

Figure 1. The thione (1a) and thiol (1b) tautomeric form of H_2L.

3.2. *Structure description*

The molecular structure of **1** is shown in figure 2. X-ray crystallography reveals that **1** consists of two crystallographically independent [CuL(phen)] units and one ethanol. The copper is surrounded by five donors in a square pyramidal fashion (4 + 1). The basal plane is made up of S, N, and O from L^{2-} and one N from phen, while the other N from phen occupies the apical position. The overall geometry is similar to that found in the corresponding complex with thiosemicarbazone [35]. Cu1 and Cu2 are similar, only having small differences in bond lengths and angles.

Selected bond lengths and angles in **1** are shown in table 2. The large difference of the two Cu-N distances for phen (2.025(5) and 2.046(4) Å in the basal plane, and 2.292(5) and 2.262(5) Å in apical position for Cu1 and Cu2, respectively) can be attributed to a Jahn–Teller distortion and rigid construction of phen. The Cu–S distances (2.249(2) and

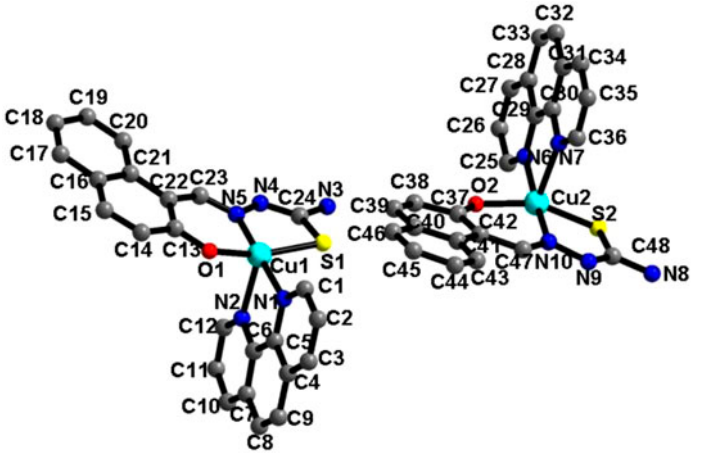

Figure 2. Ball-and-stick representation of the molecular structure of **1**; atoms are shown as spheres of arbitrary diameter, all hydrogen atoms and ethanol molecule are omitted for clarity.

Table 2. Selected bond lengths (Å) and angles (°) in **1**.

Cu(1)–O(1)	1.933(4)	Cu(1)–N(5)	1.953(4)
Cu(1)–N(1)	2.025(5)	Cu(1)–S(1)	2.249(2)
Cu(1)–N(2)	2.292(5)	Cu(2)–O(2)	1.937(4)
Cu(2)–N(10)	1.947(4)	Cu(2)–N(6)	2.046(4)
Cu(2)–N(7)	2.262(5)	Cu(2)–S(2)	2.271(2)
C(23)–N(5)	1.288(6)	C(24)–N(4)	1.301(7)
C(24)–S(1)	1.756(6)	C(47)–N(10)	1.293(6)
C(48)–N(9)	1.311(6)	C(48)–S(2)	1.740(6)
O(1)–Cu(1)–N(5)	93.17(19)	O(1)–Cu(1)–N(1)	88.64(17)
N(5)–Cu(1)–N(1)	177.61(19)	O(1)–Cu(1)–S(1)	163.29(13)
N(5)–Cu(1)–S(1)	85.67(16)	N(1)–Cu(1)–S(1)	93.03(14)
O(1)–Cu(1)–N(2)	97.20(18)	N(5)–Cu(1)–N(2)	100.74(19)
N(1)–Cu(1)–N(2)	77.5(2)	S(1)–Cu(1)–N(2)	99.39(14)
O(2)–Cu(2)–N(10)	91.86(19)	O(2)–Cu(2)–N(6)	88.63(17)
N(10)–Cu(2)–N(6)	173.3(2)	O(2)–Cu(2)–N(7)	103.15(18)
N(10)–Cu(2)–N(7)	95.92(19)	N(6)–Cu(2)–N(7)	77.5(2)
O(2)–Cu(2)–S(2)	154.54(12)	N(10)–Cu(2)–S(2)	85.34(16)
N(6)–Cu(2)–S(2)	97.04(13)	N(7)–Cu(2)–S(2)	102.30(15)

Table 3. Distances (Å) and angles (°) of hydrogen bonds for **1**[a].

D–H—A	*d*(H—A)	*d*(D—A)	∠D–H—A
O3–H3D—O2[b]	2.075	2.848	156.97
N3–H3B—N9[c]	2.147	2.979	162.50
N3–H3C—O3[d]	2.214	3.053	165.03
N8–H8B—N4[e]	2.365	3.144	150.72
N8–H8C—O1[f]	2.472	3.325	171.34

[a]Symmetry transformations used to generate equivalent atoms:
[b]#1: $x-1/2, y+1, -z+1/2$.
[c]#2: $-x, y+3/2, -z+1/2$.
[d]#3: $x-1/2, y-1, -z+1/2$.
[e]#4$-x, y-3/2, -z+1/2$.
[f]#5: $x+1/2, y, -z+½$.

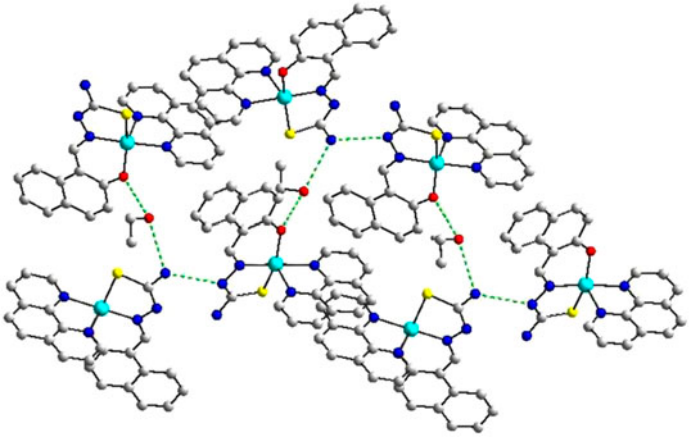

Figure 3. 1-D zigzag chain of **1**.

2.271(2) Å) are approximately equal to those reported for similar complexes, while C–S distances (1.756(6) and 1.740(6) Å) appear to be longer than those reported for free thiosemicarbazones (1.659 Å) [36]. This lengthening of C–S bonds is attributed to the enethiolization that occurs prior to coordination of the ligands with copper(II). The Cu–N, Cu–O, and Cu–S bond lengths are all very similar in the two units.

The tridentate L^{2-} is practically planar and orthogonal to phen with dihedral angles of 85.7 and 85.8° for **1**. Each H_2L coordinates with copper(II) to form two chelate rings, one six-membered and one five-membered chelate ring [Cu(1)–O(1)–C(13)–C(22)–C(23)–N(5), Cu(2)–O(2)–C(37)–C(42)–C(47)–N(10), Cu(1)–S(1)–C(24)–N(4)–N(5), and Cu(2)–S(2)–C(48)–N(9)–N(10)], which are individually almost planar with the dihedral angle of 13.7 and 13.0°. Each phen coordinates with copper to form a five-membered chelate ring [Cu(1)–N(1)–C(5)–C(6)–N(2) and Cu(2)–N(6)–C(29)–C(30)–N(7)], which is nearly perpendicular to the other two chelate rings with dihedral angles of 83.6, 95.6, 96.3, and 80.8°. Through intermolecular hydrogen bonds O–H···O, N–H···N, and N–H···N, the structure units serving as the basic building blocks are assembled into a highly ordered 1-D zigzag chain along the *b*-axis (table 3 and figure 3).

3.3. *FT-IR spectra*

FT-IR spectra data of H_2L and **1**–**4** provide useful information about metal–ligand bonding. The assignments are based on typical group frequencies. The free Schiff base exhibits a sharp peak at 3444 cm^{-1}, assigned to ν(N–H). A middle peak at 3258 cm^{-1} due to hydrogen-bonded O–H in H_2L was not observed in **1**–**4**, suggesting that the naphthol oxygen is deprotonated and coordinated in the complexes. The strong ν(C=N) peaks at 1607–1663 cm^{-1} for these complexes shift considerably compared to that of H_2L (1608 cm^{-1}), indicating that the azomethine nitrogens are also coordinated [36].

Weak peak at 480–494 cm^{-1} can be assigned to ν(M–O) and provides further evidence for coordination through deprotonated naphthol oxygen. Comparing with **1**–**4**, the FT-IR spectrum of H_2L does not exhibit a ν(SH) at 2705 cm^{-1}, but shows a peak at 3162 cm^{-1} attributable to ν(NH), indicating that in the solid state, it remains as the thione form (figure 2). However, it quickly converts to the thiol form and coordinates to metal in its deprotonated thiolate form in solution in the presence of metal(II) salts, substantiated by the disappearance of the corresponding bands for ν(SH) and ν(NH) in **1**–**4**. Metal-thiosemicarbazone complexes in which the thiosemicarbazones coordinate to a metal in their thiolate forms are reported [25–28]. For phen, bands at 1487–1533 cm^{-1} for these complexes are shifted to lower frequencies compared to free phen (1561 cm^{-1}), showing that the phen nitrogen is coordinated [37].

3.4. *UV–vis spectra*

UV–vis spectra for H_2L and **1**–**4** were obtained in DMSO : H_2O, 1 : 1 v/v. Absorptions of H_2L are at 365, 330, and 265 nm, attributed to charge transfer (CT), $n\rightarrow\pi^*$, and $\pi\rightarrow\pi^*$ transitions, respectively. Strong peaks at 405–430 nm for **1**–**4** shift considerably compared to H_2L (365 nm), implying that the ligand is coordinated. In addition, an absorption at 330 nm in **1**–**3** may be associated with charge transfer and/or $n\rightarrow\pi^*$ transitions [38]. For **3**, intense higher-energy peaks at 260 nm can be attributed to intraligand $\pi\rightarrow\pi^*$ transitions [8].

3.5. *Pharmacology*

The results of urease inhibition are summarized in table 4. H_2L and phen have very weak ability to inhibit urease. **1**, **3,** and **4** displayed potential inhibitory activities against *jack bean* urease, compared with the reference inhibitor acetohydroxamic acid. Generally, metal ions are believed to inhibit urease by binding to the sulfhydryl groups of cysteines, and possibly nitrogen–(histidine) and oxygen–(aspartic and glutamic acids) in the urease active sites [15, 39–42]. Inhibitory efficiency of metal ions against urease follows the order: $Cu^{2+} > Ni^{2+} > Co^{2+} > Zn^{2+}$, which has been reported [16, 43]. Free copper(II) ions showed strong urease inhibitory effect ($IC_{50} = 0.37\ \mu M$), because of its interactions with the urease active site [43]. The ability to inhibit urease follows the order: **3** > **4** > **1** > **2**, which is different from that of metal ions toward urease, suggesting that ligands can change the inhibition of metal ions. The most potent activity was observed in **3** with $IC_{50} = 1.2\ \mu M$; nickel(II) complex **3** is more active than copper(II) complex **1** despite containing the same ligands. The observation is different from previously reported Shiff base complexes [8, 15, 16]. Compared with other copper(II) complexes previously reported [15, 45–47], **1** exhibits weaker urease inhibitory activity. On the contrary, **3** shows stronger

Table 4. Inhibition of urease by the tested materials.

The tested materials	IC_{50} (μM)
Phen	/ [c]
H_2L	/
Cu^{2+}	0.37 ± 0.2
Zn^{2+}	/
Ni^{2+}	2.87 ± 0.4
Co^{2+}	/
1	18.3 ± 1.6
2	/
3	1.2 ± 0.1
4	10.4 ± 0.7
Acetohydroxamic acid	42.1 ± 0.4

[c]/means no inhibition activity against *jack bean* urease.

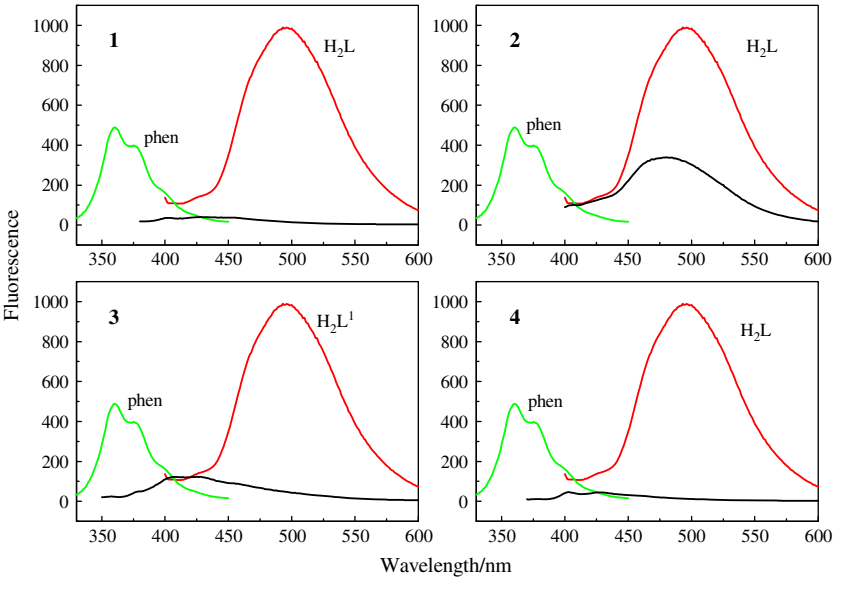

Figure 4. The fluorescence emission spectra of **1–4** and the ligands in DMSO/H_2O solution.

urease inhibitory activity than similar nickel(II) complexes [15, 16, 48]. The results show that the inhibitory efficiency of these complexes toward urease should be influenced by transition metals and by ligands.

3.6. *Fluorescence property*

The fluorescence properties of the complexes and the free ligands were measured in a solution at room temperature. As shown in figure 4, intense emissions are observed at 495 and 359 nm (λ_{ex} = 395 and 322 nm) for H_2L and phen, respectively, attributed to $\pi \rightarrow \pi^*$ charge transitions [44]. Maximum emissions of **1–4** were exhibited at 425–480 nm, blue-shifted compared with that of H_2L (λ_{em} = 395 nm). This suggests that free ligands coordinated with metal ions. For **1**, **3,** and **4**, the fluorescence intensity is weakened or

even quenched. The emission peak of **2** is at 480 nm, attributed to neither metal-to-ligand charge transfer nor ligand-to-metal charge transfer, because Zn(II) ions are d^{10} and difficult to oxidize or reduce [49, 50]. Therefore, the emission observed in **2** is attributed to the $\pi \rightarrow \pi^*$ intraligand photoluminescence due to its resemblance to that of H_2L.

4. Conclusion

Synthesis, luminescence, and urease inhibitory activities of structurally similar coordination complexes with the tridentate NOS-donor Schiff base have been described. Free H_2L has better fluorescence, but fluorescence properties of the transition metal complexes decrease. Complex 3 has the strongest inhibitory activity against *jack bean* urease, suggesting potential application as a urease inhibitor. Complex **3** has more *in vitro* inhibitory activity ($IC_{50} = 1.2\,\mu M$) than free nickel(II) ion ($IC_{50} = 2.8\,\mu M$), while the copper(II) complex **1** is quite the opposite. The trend in this work differs from previous studies, which might be related to different ligands. Inhibitory activity of metal ion might be controlled effectively by the coordination of ligands.

Supplementary material

CCDC 898700 for **1** contains the supplementary crystallographic data for this article. These data can be obtained free of charge from The Cambridge Crystallographic Data Center via www.ccdc.cam.ac.uk/data_request/cif.

Acknowledgements

This work was financially supported by the NSF of China (21001071, 21271125, 21201116), Foundation for University Key Teacher by Henan Educational Committee (2010GGJS-157), Research Program of Foundation and Advanced Technology of Henan Province (122300410386, 122102210255, 132309410397) and NSF of Henan Educational Committee (2010A150018).

References

[1] N.E. Dixon, C. Gazzola, R.L. Blakeley, B. Zerner. *J. Am. Chem. Soc.*, **97**, 4131 (1975).
[2] E. Jabri, M.B. Carr, R.P. Hausinger, P.A. Karplus. *Science*, **268**, 998 (1995).
[3] P.A. Karplus, M.A. Pearson, R.P. Hausinger. *Acc. Chem. Res.*, **30**, 330 (1997).
[4] S. Benini, W.R. Rypniewski, K.S. Wilson, S. Miletti, S. Ciurli, S. Mangani. *Structure*, **7**, 205 (1999).
[5] S. Benini, W.R. Rypnewski, K.S. Wilson, S. Miletti, S. Ciurli, S. Mangani. *J. Biol. Inorg. Chem.*, **5**, 110 (2000).
[6] H.L.T. Mobley, M.D. Island, R.P. Hausinger. *Microbiol. Rev.*, **59**, 451 (1995).
[7] Z. Amtul, M. Rasheed, M.I. Choudhary, S. Rosanna, K.M. Khan, A. Rahman. *Biochem. Biophys. Res. Commun.*, **319**, 1053 (2004).
[8] Y.G. Li, D.H. Shi, H.L. Zhu, H. Yan, S.W. Ng. *Inorg. Chim. Acta*, **360**, 2881 (2007).
[9] Z.P. Wang, O. Van Cleemput, P. Demeyer, L. Baert. *Biol. Fertil. Soils*, **11**, 41 (1991).
[10] B. Krajewska. *J. Mol. Catal. B: Enzym.*, **59**, 9 (2009).
[11] Z. Amtul, A. Rahman, R.A. Siddiqui, M.I. Choudhary. *Curr. Med. Chem.*, **9**, 1323 (2002).
[12] S. Vassiliou, P. Kosikowska, A. Grabowiecka, A. Yiotakis, P. Kafarski, Ł. Berlicki. *J. Med. Chem.*, **53**, 5597 (2010).

[13] O.R. Abid, T.M. Babar, F.I. Ali, S. Ahmed, A. Wadood, N.H. Rama, R. Uddin, Z. Haq, A. Khan, M.I. Choudhar. *ACS Med. Chem. Lett.*, **1**, 145 (2010).
[14] Z.L. You, D.M. Xian, M. Zhang, X.S. Cheng, X.F. Li. *Bioorg. Med. Chem.*, **20**, 4889 (2012).
[15] X.W. Dong, Y.G. Li, Z.W. Li, Y.M. Cui, H.L. Zhu. *J. Inorg. Biochem.*, **108**, 22 (2012).
[16] W. Chen, Y.G. Li, Y.M. Cui, X. Zhang, H.L. Zhu, Q.F. Zeng. *Eur. J. Med. Chem.*, **45**, 4473 (2010).
[17] Z.L. You, P. Zhou. *Inorg. Chem. Commun.*, **10**, 9273 (2007).
[18] K. Cheng, Q.Z. Zheng, H.L. Zhu. *Inorg. Chem. Commun.*, **12**, 1116 (2009).
[19] Z.L. You, L. Zhang, D.H. Shi, X.L. Wang, X.F. Li, Y.P. Ma. *Inorg. Chem. Commun.*, **13**, 996 (2010).
[20] N. Zhang, C.Y. Huang, D.H. Shi, Z.L. You. *Inorg. Chem. Commun.*, **14**, 1636 (2011).
[21] A.N. Kharat, A. Bakhoda, G. Bruno, H.A. Rudbari. *Polyhedron*, **45**, 9 (2012).
[22] T. Kreybig, R. Preussmann, W. Schmidt. *Arzneim.-Forsch*, **18**, 645 (1968).
[23] M.J. Domínguez, C. Sanmartín, M. Font, J.A. Palop, S.S. Francisco, O. Urrutia, F. Houdusse, J. Garcića-Mina. *J. Agric. Food Chem.*, **56**, 3721 (2008).
[24] Z.L. You, D.H. Shi, J.C. Zhang, Y.P. Ma, C. Wang, K. Li. *Inorg. Chim. Acta*, **384**, 54 (2012).
[25] X.Y. Qiu, S.Z. Li, A.R. Shi, Q.Q. Li, B. Zhai. *Chin. J. Struct. Chem.*, **31**, 555 (2012).
[26] X.Y. Qiu, Q.F. Liu, P. Zhang, L.Q. Sheng. *Chin. J. Inorg. Chem.*, **28**, 362 (2012).
[27] X.Y. Qiu, M.A. Zhu, Y. Liu, X.Y. Ding, P. Zhang. *Chin. J. Struct. Chem.*, **29**, 1557 (2010).
[28] X.Y. Qiu, Y. Liu, Y. Chen, X. Zheng, H.L. Zhu. *Chin. J. Inorg. Chem.*, **26**, 1485 (2010).
[29] X.Y. Qiu, M.A. Zhu, M.W. Zhang, M.T. Xu, H.L. Zhu. *Chin. J. Struct. Chem.*, **29**, 806 (2010).
[30] G.M. Sheldrick. *SHELXTL V5.1 software reference manual*, Bruker AXS, Madison, WI (1997).
[31] T. Tanaka, M. Kawase, S. Tani. *Life Sci.*, **73**, 2985 (2003).
[32] W. Zaborska, B. Krajewska, Z. Olech. *J. Enzyme Inhib. Med. Chem.*, **19**, 65 (2004).
[33] D.D. Van Slyke, R.M. Archibald. *J. Biol. Chem.*, **154**, 623 (1944).
[34] H.C. Fang, X.Y. Yi, Z.G. Gu, G. Zhao, Q.Y. Wen, J.Q. Zhu, A.W. Xu, Y.P. Cai. *Cryst. Growth Des.*, **9**, 3776 (2009).
[35] M. Baldini, M. Belicchi-Ferrari, F. Bisceglie, G. Pelosi, S. Pinelli, P. Tarasconi. *Inorg. Chem.*, **42**, 2049 (2003).
[36] X.X. Zhou, Y.P. Cai, S.Z. Zhu, Q.G. Zhan, M.S. Liu, Z.Y. Zhou, L. Chen. *Cryst. Growth Des.*, **8**, 2076 (2008).
[37] Y.L. Zhao, F.Y. Zhao. *J. Chin. Rare Earth Soc.*, **19**, 398 (2001).
[38] U. Mukhopadhyay, L.R. Falvello, D. Ray. *Eur. J. Inorg. Chem.*, **11**, 2823 (2001).
[39] B. Krajewska. *J. Enzyme Inhib. Med. Chem.*, **23**, 535 (2008).
[40] B. Krajewska, W. Zaborska, M. Chudy. *J. Inorg. Biochem.*, **98**, 1160 (2004).
[41] W. Zaborska, B. Krajewska, M. Leszko, Z. Olech. *J. Mol. Catal. B: Enzym.*, **13**, 103 (2001).
[42] C. Follmer, C.R. Carlini. *Arch. Biochem. Biophys.*, **435**, 15 (2005).
[43] B. Krajewska. *J. Chem. Technol. Biotechnol.*, **52**, 157 (1991).
[44] Z.M. Chen, J.L. Zou, Y.Q. Yang, D.Z. Kuang, J.Q. Wang, F.X. Zhang, M.S. Chen. *Chin. J. Inorg. Chem.*, **27**, 2167 (2011).
[45] Y.G. Li, Z.W. Li, Y. Liu, X.W. Dong, Y.M. Cui. *J. Coord. Chem.*, **65**, 19 (2012).
[46] Y.M. Cui, W.T. Liu, Y. Liu, W. Chen, Y.G. Li. *J. Coord. Chem.*, **64**, 3960 (2011).
[47] L. Sun, Y.G. Li, X.W. Dong, M.X. Guo. *Transition Met. Chem.*, **37**, 361 (2012).
[48] Y. Lu, D.H. Shi, Z.L. You, X.S. Zhou, K. Li. *J. Coord. Chem.*, **65**, 339 (2012).
[49] U.H.F. Bunz. *Chem. Rev.*, **100**, 1605 (2000).
[50] W.Y. Yang, H. Schmider, Q.G. Wu, Y.S. Zhang, S. Wang. *Inorg. Chem.*, **39**, 2397 (2000).